

Theoretical Studies of Hetero-Diels–Alder Reactions Involving *N*-Sulfinyl Dienophiles

Young Sook Park,[†] Wang Ki Kim,[†] Yong Bin Kim,[†] and Ikchoon Lee*[‡]

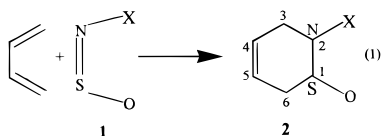
Department of Chemical Education, Chonnam National University, Kwangju, 500-757 Korea, and
Department of Chemistry, Inha University, Incheon, 402-751 Korea

Received December 28, 1999

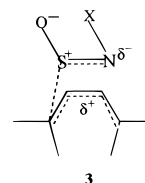
The gas-phase hetero-Diels–Alder reactions between butadiene and X-substituted sulfinyl dienophiles, O[−]–S⁺=N–X, are investigated theoretically at the B3LYP/6-31G* level. The *Z*-forms of the dienophiles are found to be more stable (by 5–7 kcal mol^{−1}) than the *E*-forms. Four modes of cycloadducts are considered: *Z-endo*; *Z-exo*; *E_{X-endo}*; *E_{X-exo}*. Five factors are responsible for the decreasing energetic preferences of the adducts in the order *E_{X-endo}* > *E_{X-exo}* > *Z-endo* > *Z-exo*: (i) The σ–σ* proximate charge-transfer interactions in the TS; (ii) the relative sizes of the LUMO AO coefficients on S and N atoms; (iii) steric hindrance in the TS; (iv) the levels of the ground state and the LUMOs of the dienophile; (v) bond energies of the C–S and C–N bonds that are formed in the TS. All the reactions proceed concertedly, but the adduct formation is asynchronous. The *endo*-additions are favored over the *exo*-additions kinetically (lower Δ*G*[‡]) as well as thermodynamically (lower Δ*G*[°]). The major secondary orbital interaction determining the *endo* preference is that between the lone pair on N (n_N) and the d₃ (C₃–C₄) σ* orbital (n_N–σ*_{d3}) interactions, whereas the larger AO lobe (LUMO) sizes on S favor a greater degree of d₅ (C–S) bond formation than d₆ (C–N) bond. The solvent, C₆H₆, uniformly lowers the activation barriers so that the energetic preferences in the gas phase between various modes are maintained in solution.

Introduction

Diels–Alder cycloadditions with a variety of *N*-sulfinyl compounds, **1**, where X = Ar, SO₂Ar, COR, CN, etc., have provided a valuable synthetic means for heterocyclic ene compounds,¹ 3,6-dihydro-1,2-thiazine 1-oxide, **2** (eq 1).

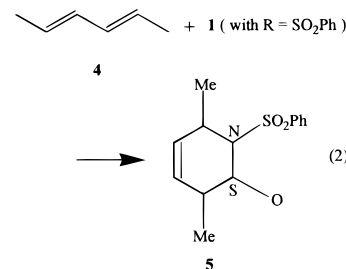


These *N*-sulfinyl Diels–Alder reactions are known to proceed quite rapidly provided that the *N*-sulfinyl compound, **1**, has an electron-withdrawing group X on nitrogen.^{1c,d} Two different mechanisms^{1c,d} have been proposed for this reaction, eq 1: (i) a nonconcerted stepwise mechanism in which the electrophilic sulfur atom of **1** adds initially to form a dipolar intermediate,² **3**; (ii) a concerted cycloaddition which is consistent with FMO theory.³ The *N*-sulfinyl compounds such as **1** are known to exist in their ground states as the *Z* geometric isomers, but it has not been possible to determine



unambiguously whether the *Z* isomer or a transient *E* isomer is the reactive species in the cycloaddition.^{1d} For some *N*-sulfinylamines, an *E/Z* equilibrium has been observed in solution.⁴

The major product in the cycloaddition of 2,4-hexadiene, **4**, with *N*-sulfinylarylsulfonamides (**1** with X = SO₂-Ph), eq 2, corresponded to *endo* addition² where the



sulfinyl oxygen and X (=SO₂Ph) are placed in proximity of the π-electron density of diene **4**. Thus there is a possibility of secondary orbital interactions between the diene π-orbitals and the S–O and N–X bonds in the TS of a concerted cycloaddition.⁵ To elucidate such mecha-

[†] Chonnam National University.

[‡] Inha University. Tel: +82-32-860-7671. Fax: +82-32-865-4855. E-mail: ilee@dragon.inha.ac.kr. Tel: +82-32-860-7671. Fax: +82-32-865-4855. E-mail: ilee@dragon.inha.ac.kr.

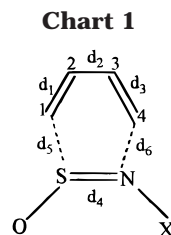
(1) (a) Kresze, G. In *1,4-Cycloaddition Reactions, the Diels–Alder Reaction in Heterocyclic Syntheses*, Hamer, J., Ed.; Academic Press: New York, 1967; p 453. (b) Weinreb, S. M.; Staib, R. R. *Tetrahedron* **1982**, *38*, 3087. (c) Boger, D. L.; Weinreb, S. M. *Hetero Diels–Alder Methodology in Organic Synthesis*, Academic Press: San Diego, CA, 1987. (d) Weinreb, S. M. *Acc. Chem. Res.* **1988**, *21*, 313. (e) Carruthers, W. *Cycloaddition Reactions in Organic Synthesis*; Pergamon Press: U.K., Oxford, 1990; Vol. 8, Chapter 1.

(2) Mock, W. L.; Nugent, R. M. *J. Am. Chem. Soc.* **1975**, *97*, 6521, 6526.

(3) (a) Hanson, P.; Stockburn, W. A. *J. Chem. Soc., Perkin Trans. 2* **1985**, 589. (b) Zhang, Y.; Flann, C. J. *J. Org. Chem.* **1998**, *63*, 1372.

(4) (a) Beagley, B.; Chantrell, S. J.; Kirby, R. G.; Schindling, D. G. *J. Mol. Struct.* **1975**, *25*, 319. (b) Kresze, G.; Berger, M.; Claus, P. K.; Rieder, W. *Org. Magn. Reson.* **1976**, *8*, 170. (c) Yavari, I.; Staral, J. S.; Roberts, J. D. *Org. Magn. Reson.* **1979**, *12*, 340.

(5) Fleming, I. *Frontier Orbitals and Organic Chemical Reactions*; John Wiley: London, 1976; Chapter 4.



nistic aspects, we undertook MO theoretical studies on the *N*-sulfinyl Diels–Alder reactions, eq 1, with X = CH₃, H, Cl, CN, and NO₂. In view of our previous success with the theoretical studies on the hetero-Diels–Alder reactions using the density functional theory (DFT),⁶ we kept our computations at the B3LYP/6-31G* level. Our primary goal in the present work is to elucidate the mechanism of the *N*-sulfinyl Diels–Alder reactions, eq 1, specifically (i) by providing theoretical basis for the concerted mechanism, (ii) by deciding whether the *Z* or a transient *E* isomer is the reactive species of *N*-sulfinyl dienophiles, (iii) by determining whether there is secondary orbital interactions in the transition state (TS) of the preferred *endo* cycloaddition, and (iv) last by examining the effect of substituent X (= CH₃, H, Cl, CN, NO₂) on the N atom of the *N*-sulfinyl dienophile on the reactivity.

Computational Method

The calculations were conducted with the Gaussian 98 program⁷ at the theoretical level of B3LYP/6-31G*//B3LYP/6-31G*.⁸ The stationary states were confirmed by calculation of the vibrational frequencies at the B3LYP/6-31G* level. The gas-phase standard free energy and activation free energy changes, ΔG° and ΔG^\ddagger , relative to the separated reactants were obtained by applying zero-point (ZPE) and thermal energy corrections and entropy changes, ΔS° and ΔS^\ddagger , to the calculated energies (ΔE° and ΔE^\ddagger). Natural bond orbital (NBO) analyses⁹ were carried out to calculate the proximate σ – σ^* secondary orbital interactions. The solvation energies ($\Delta G_{\text{sol}}^\circ$) in benzene ($\epsilon = 2.28$) were calculated using the isodensity polarizable continuum model IPCM¹⁰ with the isodensity level of 0.0004 au. The numbering of the atoms and bonds in the adduct is shown in Chart 1.

(6) Park, Y. S.; Lee, B.-S.; Lee, I. *New J. Chem.* **1999**, *23*, 707.

(7) Frisch, M. J.; Trucks, G. W.; Schlegel, H. B.; Scuseria, G. E.; Robb, M. A.; Cheeseman, J. R.; Zakrzewski, V. G.; Montgomery, J. A.; Stratmann, R. E.; Burant, J. C.; Dapprich, S.; Millam, J. M.; Daniels, A. D.; Kudin, K. N.; Strain, M. C.; Farkas, O.; Tomasi, J.; Barone, V.; Cossi, M.; Cammi, R.; Mennucci, B.; Pomelli, C.; Adamo, C.; Clifford, S.; Ochterski, J.; Petersson, G. A.; Ayala, P. Y.; Cui, Q.; Morokuma, K.; Malick, D. K.; Rabuck, A. D.; Raghavachari, K.; Foresman, J. B.; Cioslowski, J.; Ortiz, J. V.; Stefanov, B. B.; Liu, G.; Liashenko, A.; Piskorz, P.; Komaromi, I.; Gomperts, R.; Martin, R. L.; Fox, D. J.; Keith, T.; Al-Laham, M. A.; Peng, C. Y.; Nanayakkara, A.; Gonzalez, C.; Challacombe, M.; Gill, P. M. W.; Johnson, B. G.; Chen, W.; Wong, M. W.; Andres, J. L.; Head-Gordon, M.; Replogle, E. S.; Pople, J. A. *Gaussian 98*, Revision A.1; Gaussian, Inc.: Pittsburgh, PA, 1998.

(8) The density functional theory method B3LYP is a hybrid functional made up of Becke's exchange functional, the Lee–Yang–Parr correlation functional, and a Hartree–Fock exchange term: (a) Becke, A. D. *J. Chem. Phys.* **1993**, *98*, 5648. (b) Becke, A. D. *J. Chem. Phys.* **1996**, *104*, 1040. (c) Becke, A. D. In *Modern Electronic Structure Theory*; Yarkony, D. R., Ed.; World Scientific: Singapore, 1995.

(9) (a) Reed, A. E.; Curtiss, L. A.; Weinhold, F. *Chem. Rev.* **1988**, *88*, 899. (b) Epitotis, N. D.; Cherry, W. R.; Shaik, S.; Yates, R.; Bernardi, F. *Structural Theory of Organic Chemistry*; Springer-Verlag: Berlin, 1977; Part IV. (c) Glendening, E. D.; Weinhold, F. *J. Comput. Chem.* **1998**, *19*, 593, 610. (d) Glendening, E. D.; Badenhop, J. K.; Weinhold, F. *J. Comput. Chem.* **1998**, *19*, 628.

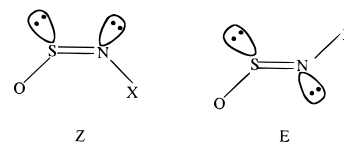
(10) Foresman, J.; Keith, T. A.; Wiberg, K. B.; Snoonian, J.; Frisch, M. J. *Phys. Chem.* **1996**, *100*, 16098. (b) Wiberg, K. B.; Rablen, P. R.; Keith, T. A. *J. Am. Chem. Soc.* **1995**, *117*, 4261. (c) Rablen, P. R.; Pearlman, S. A.; Miller, D. A. *J. Am. Chem. Soc.* **1999**, *121*, 227.

Table 1. Comparison of Stabilities, $\Delta G(E-Z)$, of the Two Forms of Sulfinyl Dienophiles and Rotational Barriers around the S=N Bond, $\Delta G_{\text{rot}}(\text{TS}-Z)$, at the B3LYP/6-31G* Level

X	$\Delta G(E-Z)$ (kcal mol ⁻¹)	$\Delta G_{\text{rot}}(\text{TS}-Z)$ (kcal mol ⁻¹)	X	$\Delta G(E-Z)$ (kcal mol ⁻¹)	$\Delta G_{\text{rot}}(\text{TS}-Z)$ (kcal mol ⁻¹)
CH ₃	7.2	16.2	CN	4.2	
H	5.3	17.1	NO ₂	3.5	18.9
Cl	7.0				

Results and Discussion

Sulfinyl Dienophiles. The two forms, *E* and *Z*, are possible with the sulfinyl dienophiles. Although experi-



mentally the *Z* form is thought to be more stable and hence is the reacting species, it has never been determined unambiguously.^{1d} We have compared stabilities of the two forms and the rotational barriers around the S=N bond in Table 1. We note that in all cases the *Z* form is more stable in agreement with the experimental evidence¹¹ but as the X substituent becomes more electron-withdrawing the energy difference, ΔE , decreases, from 6.8 kcal mol⁻¹ for X = CH₃ to 4.6 kcal mol⁻¹ for X = NO₂. This *Z* over *E* preference is dictated by the dominant interaction of the n – σ^* vicinal overlap, which is maximized in a *Z* arrangement; i.e., the vicinal n – σ^* interactions, $n_{\text{N}}-\sigma_{\text{SO}}^*$ and $n_{\text{S}}-\sigma_{\text{NX}}^*$, are greater when the two, n and σ^* , are trans to each other.^{9b} When, however, the n – σ^* interactions become weak due to a strong electron-withdrawing effect of X (σ_{NX}^* becomes a weaker acceptor when X is more electron rich), the *E* form becomes more favorable due partially to lesser steric hindrance between O and X.^{9b} On the other hand, dipole moments are 1.67, 0.80, 0.92, 3.54, and 2.70 D for *Z* forms but they are 3.74, 3.44, 2.34, 2.47 and 1.83 D for *E* forms in the order X = CH₃, H, Cl, CN, and NO₂, respectively. The inversion of stability order from *Z* preference (for X = CH₃, H, and Cl) to *E* preference (X = CN and NO₂) becomes apparent from these dipole moment data.

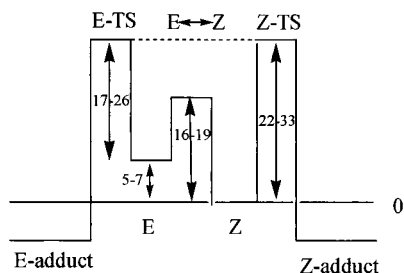
The rotational barriers are high, 16–19 kcal mol⁻¹, so that equilibration by rotation around S=N bond is practically prohibited.⁴ We therefore conclude that although the difference in stabilities of the two forms are small, the sulfinyl dienophiles should be in *Z* forms predominantly in the ground states and the cycloadditions start from the *Z* forms. We nevertheless considered the cycloadditions by both *Z* and *E* forms of the sulfinyl dienophiles.

Transition States and Energetics. In all cases, the two bonds, d_5 and d_6 , are formed simultaneously and therefore the additions are concerted. In this respect stepwise additions are unlikely in the gas phase although we have not carried out UHF calculations. This is in contrast to a nonconcerted stepwise dipolar addition mechanism proposed by Mock et al.² The activation free

(11) (a) Caminati, W.; Mirri, A.; Macagnani, G. *J. Mol. Spectrosc.* **1977**, *66*, 368. (b) Bak, B.; Svanholt, H.; Larsen, C. *J. Mol. Struct.* **1977**, *36*, 55. (c) Beagley, B.; Chantrell, S.; Kirby, R.; Schmidling, D. *J. Mol. Struct.* **1975**, *25*, 319. (d) Gieren, A.; Deder, B. *Angew. Chem., Int. Ed. Engl.* **1977**, *16*, 179. (e) Mey, R.; Oskam, A.; Stufkens, D. *J. Mol. Struct.* **1979**, *51*, 37.

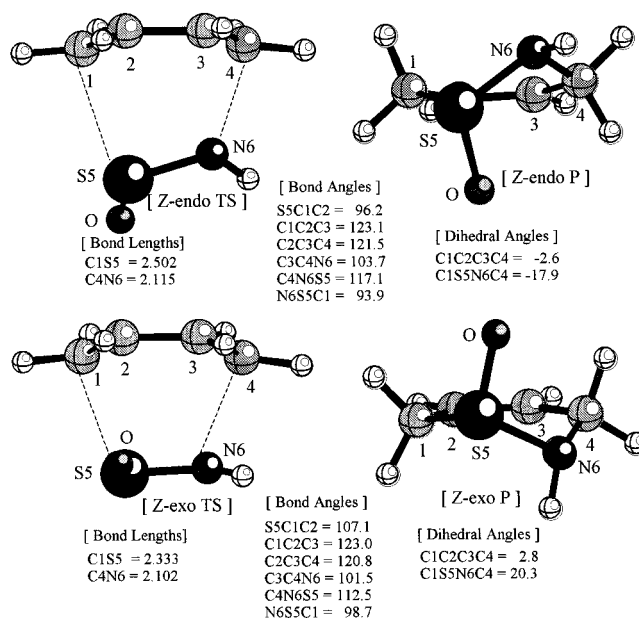
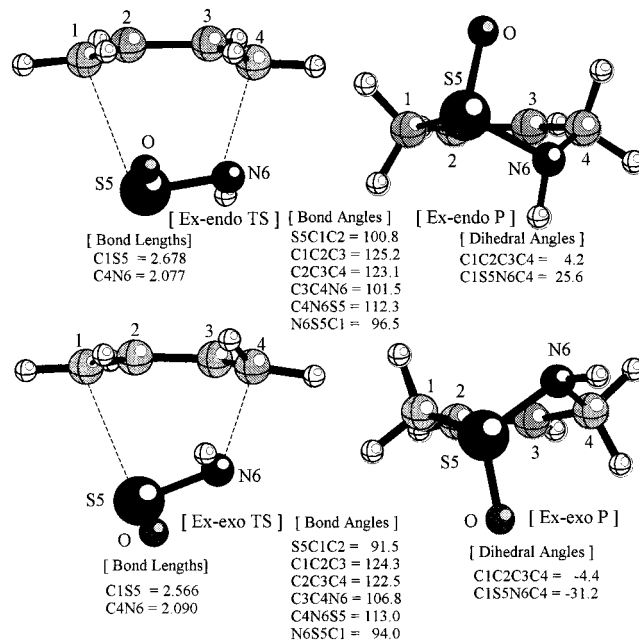
Table 2. Energetics for Various Modes of Gas-Phase Cycloaddition (kcal mol⁻¹) with *cis*-Butadiene at the B3LYP/6-31G* Level^a

	X	ΔG^\ddagger	ΔG°		X	ΔG^\ddagger	ΔG°
<i>Z-endo</i>	CH ₃	30.6	-0.1	<i>E_{X-endo}</i>	CH ₃	22.9	-3.1
	H	24.5	-3.8		H	19.2	-5.2
	Cl	27.5	-2.5		Cl	18.6	-6.5
	CN	23.8	-4.2		CN	18.2	-6.8
	NO ₂	22.4	-14.3		NO ₂	19.0	-15.3
<i>Z-exo</i>	CH ₃	33.2	4.1	<i>E_{X-exo}</i>	CH ₃	26.1	-7.3
	H	27.6	0.1		H	23.0	-9.1
	Cl	29.0	-2.5		Cl	19.5	-9.5
	CN	25.7	-4.2		CN	19.4	-8.5
	NO ₂	24.3	-10.5		NO ₂	16.9	-17.9

^a Corrected for zero-point energies.**Figure 1.** Relative energy levels of the *Z* and *E* forms in kcal mol⁻¹. *E* and *Z*-TS are the TS levels for the cycloadditions.

energies (ΔG^\ddagger) and reaction free energies (ΔG°) are summarized in Table 2 for four modes of cycloadditions, *Z-endo*, *Z-exo*, *E_{X-endo}*, and *E_{X-exo}*. In the latter two modes, the *E* form of sulfinyl dienophile forms an adduct with the X group directed toward the diene (*X-endo*) and away from the diene (*X-exo*), respectively. Reference to Table 2 reveals that, overall, the cycloaddition becomes more facile, ΔG^\ddagger decreases, and the reaction becomes more exothermic, as electron-withdrawing power of the substituent X increases. In the additions of *Z*-dienophiles, the *endo* modes are kinetically as well as thermodynamically preferred over the *exo* modes in agreement with experimental results.^{2,3} However the difference in ΔG^\ddagger between the *Z-endo* and *Z-exo* addition is reduced as the electron-withdrawing power of X becomes stronger from 2.6 kcal mol⁻¹ for X = CH₃ to 1.9 kcal mol⁻¹ for X = NO₂. The similar trends are found with the cycloadditions with the *E*-sulfinyl dienophiles. Despite the greater stabilities of the *X-exo* adducts, the *X-endo* addition mode is preferred kinetically to the *X-exo* mode, and the activation energy difference decreases with the increase in the electron-accepting power of the X substituent. Finally the preference reverses to *X-exo* with X = NO₂. This reversal of the energetic preference from *endo* for X = CH₃ to *exo* addition for X = NO₂ most probably results from the lowering of the lone-pair level on N, n_N , by an electron-withdrawing group, X, since such lowering should lead to a wider frontier MO (FMO) gap, $\Delta\epsilon_{\text{FMO}} = \epsilon_{\sigma^*} - \epsilon_n$, which in turn leads to a lower second-order charge-transfer stabilization energy¹² involved in the secondary orbital interaction between n_N and σ_{d3}^* orbital in the *endo* addition (vide infra).

It is, however, to be noted that the cycloadditions with the *E* forms are considerably more favorable (by ca. 5–9 kcal mol⁻¹) than those with the *Z* forms. The magnitude of this energy difference is similar to that between the

**Figure 2.** DFT results of the transition structures and products for *Z-endo* and *Z-exo* cycloadditions. Bond lengths are in Å, and angles are in deg.**Figure 3.** DFT results of the transition structures and products for *E_{X-endo}* and *E_{X-exo}* cycloadditions. Bond lengths are in Å, and angles are in deg.

two isomers in the ground state (5–7 kcal mol⁻¹). This means that actually the cycloadditions of *E*- and *Z*-sulfinyl dienophiles with butadiene have approximately the same transition state level, TS-*E* level \approx TS-*Z* level in Figure 1. We therefore think that the cycloadditions can occur competitively from both the *E* and *Z* ground states, although the *Z* form is more abundant and the interconversion between the *E* and *Z* forms is difficult in the ground state. But the rotational barrier is lower than the activation energy for addition so that there should be close to thermal equilibration prior to addition. The TS and product structures are shown in Figures 2 and 3. The *Z-endo* mode of cycloadditions is energetically

(12) (a) Reference 9b, Part I. (b) Fleming, I. *Frontier Orbitals and Organic Chemical Reactions*; Wiley: London, 1976; Chapter 4.

Table 3. % Δn^\ddagger for *Z-endo* Adducts^a at the B3LYP/6-31G* Level

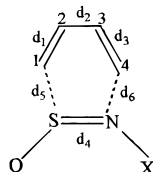
X	d_1 (% Δn^\ddagger)	d_2 (% Δn^\ddagger)	d_3 (% Δn^\ddagger)	d_4 (% Δn^\ddagger)	d_5 (% Δn^\ddagger)	d_6 (% Δn^\ddagger)
CH ₃	31.2 ^a (34.8)	39.0 (45.2)	40.0 (36.5)	52.6 (54.2)	29.3 (36.5)	41.1 (36.1)
H	31.6 (33.5)	40.0 (42.6)	38.0 (35.6)	48.8 (49.3)	32.7 (35.5)	38.0 (35.7)
Cl	36.6 (39.3)	42.5 (45.4)	38.8 (38.1)	56.4 (61.0)	36.5 (40.8)	39.1 (35.9)
CN	44.3 (45.0)	46.1 (46.9)	37.6 (36.3)	52.5 (51.6)	47.9 (48.0)	32.0 (30.5)
NO ₂	36.8 (38.7)	40.4 (43.0)	31.9 (31.3)	45.6 (46.7)	39.5 (41.5)	27.2 (27.8)

^a The values for *Z-exo* adducts are shown in the parentheses.

Table 4. Major Second-Order Proximate $\sigma-\sigma^*$ Interactions in the Transition States for *Z-endo* and *Z-exo* Cycloadditions

X	$\sigma \rightarrow \sigma^*$	$-\Delta E^{(2)}_{\sigma-\sigma^*}$ (kcal mol ⁻¹)		$-\Sigma \Delta E^{(2)}_{\sigma-\sigma^*}$ ^a	
		<i>endo</i>	<i>exo</i>	<i>endo</i>	<i>exo</i>
CH ₃	$d_1 d_4$	13.8	16.9		
	$d_4 d_1$	2.6	6.4		
	$d_3 d_4$	35.6	27.2		
	$d_4 d_3$	25.5	18.6	77.5	69.1
	$n_N d_3$	19.4	7.9		
H	$d_1 d_4$	16.8	15.3		
	$d_4 d_1$	10.6	18.0		
	$d_3 d_4$	28.6	28.7		
	$d_4 d_3$	33.9	29.5	89.9	91.5
	$n_N d_3$	13.4	5.6		
NO ₂	$d_1 d_4$	34.0	28.0		
	$d_4 d_1$	15.3	24.9		
	$d_3 d_4$	13.9	13.9		
	$d_4 d_3$	12.5	14.7	75.7	81.5
	$n_N d_3$	8.1	5.6		

^a The four d_1-d_4 and d_3-d_4 $\sigma-\sigma^*$ interaction energies are summed.



preferred over the *Z-exo* mode by 2–2.5 kcal mol⁻¹ (Table 2). To see why the *endo* additions are favored despite the obviously unfavorable steric hindrance effect, we calculated percentage bond order changes, % Δn^\ddagger ¹³ (eq 3,

$$\% \Delta n^\ddagger = \frac{[\exp(-r^\ddagger/a) - \exp(-r_R/a)]}{[\exp(-r_P/a) - \exp(-r_R/a)]} \times 100 \quad (3)$$

$$\Delta E^{(2)}_{\sigma-\sigma^*} = -\frac{2 < \sigma | F | \sigma^* >^2}{\epsilon_{\sigma\sigma^*} - \epsilon_\sigma} \quad (4)$$

where r^\ddagger , r_R , and r_P are the distances in the TS, reactant, and product and the a values are fixed to 0.3 for d_1-d_4 and to 0.6 for d_5 and d_6), and the second-order proximate $\sigma-\sigma^*$ (including $\pi-\pi^*$, $n-\pi^*$, etc.) interaction energies, $\Delta E^{(2)}_{\sigma-\sigma^*}$, using natural bond orbitals⁹ (eq 4, where F is a Fock operator) as shown in Tables 3 and 4.

Examination of Table 3 shows that the degree of bond formation in the TS is less than 50% in all cases. Thus the TS's are located early on the reaction coordinate so that the reactivity is frontier MO (FMO) controlled,^{9b,14} i.e., the activation energies are determined either by the FMO gap, $\Delta\epsilon = \epsilon_{LU} - \epsilon_{HO}$, or by the Fock matrix element, $F_{\sigma\sigma^*}$, which is proportional to the $\sigma-\sigma^*$ overlap. Both

modes of adducts (*E* and *Z*) are seen to be *asynchronous*, i.e., the degree of bond formation is not the same for d_5 (C--S) and d_6 (C₄--N). In the *endo* adducts, the steric hindrance due to the S–O bond causes to retard d_5 bond formation, but in the *exo* adducts there is no such steric effect and d_5 bond formation becomes facile and progresses ahead of d_6 . The NBO charges indicate that the S–O bond in the ground state dienophile is highly polarized to S⁺–O⁻ and the N–X bond is weakly polarized to N⁻–X⁺. Therefore C₁–S bond formation is electrostatically facilitated compared to the C₄–N bond formation in the TS since the cycloaddition is a normal electron demand type and the dienophile is an electron acceptor as the frontier MOs (FMOs) show in Table 5. The larger sizes of the LUMO AO coefficients on S than on N in Table 6 are also in favor of the greater (C₁–S) d_5 than (C₄–N) d_6 bond formation. In the absence of steric hindrance and secondary orbital overlap interaction ($n_N-\sigma^*_{d3}$) as in the *Z-exo* addition, bond formation of C₁–S becomes more facile than that of C₄–N and takes place ahead of C₄–N bond (Table 3). This type of mechanism in which the TS is formed by initial C–S bond formation has been proposed by Mock and Nugent.² However there are two factors in favor of the *endo* adduct than *exo*-adduct formation: (i) The bond energy is greater for C–N (73 kcal mol⁻¹) than C–S (65 kcal mol⁻¹).¹⁵ (ii) The secondary orbital interactions between diene and dienophile in the TS⁵ are greater in the *endo* than *exo* adduct. These secondary orbital interactions of the proximate $\sigma-\sigma^*$ types are in favor of the *endo* adducts (Table 4) for X = CH₃ and H but reverse in favor of *exo* adducts for X = NO₂. However, the charge transfer of the nitrogen lone pair (n_N) toward the d_3 σ^* bond orbital (σ^*_{d3}) is in favor of the *endo* adduct in all cases. This could be the main reason the *endo* adduct is favored over the *exo* adduct despite the larger steric hindrance due to the S–O and N–X bonds. In the *endo* adduct the steric effect is partially alleviated by a skewed approach of the dienophile in which O and X point upward and S–O and N–X are tilted away from the diene molecular plane (Figures 2 and 3). In this type of approach the n_N-d_3 orbital interaction is also maximized (Figure 4).

In the *endo* adducts the progress of d_6 bond making (38–41%) is ahead of d_5 (29–37%) in the TS for X = CH₃, H, and Cl but reverses to a more advanced d_5 bond formation than d_6 for X = CN and NO₂, whereas in the *exo* adducts that of d_5 (41–48%) is ahead of d_6 (28–36%) for X = Cl, CN, and NO₂ but almost synchronous for X = CH₃ and H (~36%). This may be due partly to a greater steric hindrance of S–O toward d_1 than N–X toward d_3 in the *endo* adduct formation. As discussed above, the secondary orbital interaction, $n_N-\sigma^*_{d3}$, seems to play an important role in the *endo* addition. $n_N-\sigma^*_{d3}$ charge-transfer interaction favors d_6 bond formation, but as the electron-withdrawing power of substituent X increases, this preference decreases due to wider FMO gap, $\Delta\epsilon_{FMO} = \epsilon_{\sigma^*} - \epsilon_n$, and other effects, e.g. AO coefficients of the

(13) (a) Houk, K. N.; Gustabson, S. M.; Black, K. A. *J. Am. Chem. Soc.* **1992**, *114*, 8565. (b) Lee, I.; Kim, C. K.; Lee, B. S. *J. Comput. Chem.* **1995**, *16*, 1045. (c) Lee, J. K.; Kim, C. K.; Lee, I. *J. Phys. Chem. A* **1997**, *101*, 2893.

(14) Klumpp, G. W. *Reactivity in Organic Chemistry*; Wiley: New York, 1982; p 370.

Table 5. Frontier Molecular Orbital Levels Calculated at the HF/6-31G/B3LYP/6-31G* Level (ϵ in au)**

X	normal electron demand ^a			reverse electron demand		
	diene HOMO	dienophile LUMO	$\Delta\epsilon_{\text{FMO}}$	diene LUMO	dienophile LUMO	$\Delta\epsilon_{\text{FMO}}$
CH ₃	-0.322 38	0.042 50	0.36	0.127 26	0.405 98	0.53
H	-0.322 38	0.032 84	0.36	0.127 26	-0.435 03	0.56
Cl	-0.322 38	0.006 74	0.33	0.127 26	-0.417 08	0.54
CN	-0.322 38	-0.036 69	0.29	0.127 26	-0.426 13	0.55
NO ₂	-0.322 38	-0.022 17	0.10	0.127 26	-0.470 18	0.60

^a The reactivities based on ΔG^\ddagger (Table 2) are consistent with normal electron demand cycloadditions.

Table 6. π^* LUMO AO Coefficients and Levels of N-Sulfinyl Dienophiles (Z Forms) at the HF/6-31G/B3LYP/6-31G* Level**

X	ratio $p_z(\text{S})/p_z(\text{N})$	S: 3p _z 4p _z	N: 2p _z 3p _z	LUMO level (au)
CH ₃	1.23	0.52, 0.52	-0.37, -0.48	0.043
H	1.28	0.54, 0.53	-0.35, -0.48	0.033
Cl	1.25	0.54, 0.50	-0.37, -0.47	0.007
CN	1.58	0.55, 0.47	-0.30, -0.35	-0.037
NO ₂	1.39	0.56, 0.50	-0.36, -0.40	-0.022

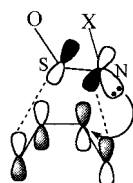


Figure 4. TS for *Z-endo* addition. A secondary orbital interaction of $n_{\text{N}}-\sigma^*_{\text{d}_3}$ is possible. The S–O and N–X bonds are tilted upward to alleviate steric hindrance, and the lone pair on N (n_{N}) can point downward partially to interact with the σ^* orbital of the d_3 ($\text{C}_3\text{--}\text{C}_4$) double bond.

LUMO on S and N, become more important and d_5 bond formation begins to be favored. In contrast in the *exo* addition, the advantage of larger LUMO lobe size on S diminishes as the electron-withdrawing power of substituent X decreases, as the low ratio of $p_z(\text{S})/p_z(\text{N})$ (=1.23) in Table 6 suggests.

The FMO energy gaps, $\Delta\epsilon = \epsilon_{\text{dienophileLUMO}} - \epsilon_{\text{dieneHOMO}}$, in Table 5, decrease as the electron-withdrawing power of X substituent in the dienophile increases from X = CH₃ to X = NO₂ due to lowering of the LUMO level by an electron-accepting X group. Therefore, the activation barriers, ΔE^\ddagger and ΔG^\ddagger , are in the decreasing order. $\Delta G^\ddagger(\text{X})$: CH₃ (>Cl) > H > CN > NO₂ (Table 2). The anomalous behavior of X = Cl may be due to the weak π -donor effect of the Cl substituent.¹⁶ The AO coefficients of the π^* -type LUMO in the sulfinyl dienophiles are shown in Table 6 together with the LUMO levels for the *Z* forms. We note that the AO coefficients are larger on the S than on the N atom, the ratio of $p_z(\text{S})/p_z(\text{N})$ being greater than 1.0 in all cases which increases as the electron-withdrawing power of X substituent increases (except for X = CN). This means that under the same conditions bond formation of S with C₁ is favored over that of N with C₄. This is reflected on the greater degree of d_5 bond formation than d_6 in the *Z-exo* adducts.

Reference to Table 4 shows that as the electron-withdrawing power of X increases, the *endo* preference over the *exo* addition due to $\sigma-\sigma^*$ orbital interactions decreases. This may be ascribed again to a decrease in the secondary orbital interaction ($n_{\text{N}}-\sigma^*_{\text{d}_3}$), which leads

Table 7. Solvation Energies in Benzene for the Adducts at the B3LYP/6-31G* Level (kcal mol⁻¹)

	X	$\Delta G^\ddagger_{\text{sol}}^a$	$\Delta G^\circ_{\text{sol}}^b$
<i>Z-exo</i>	CH ₃	32.8	3.2
	H	27.2	-0.8
	Cl	28.5	-3.5
	CN	24.2	-5.6
	NO ₂	23.1	-12.4
<i>Z-endo</i>	CH ₃	30.4	-0.9
	H	24.1	-4.6
	Cl	26.9	-3.5
	CN	22.3	-5.6
	NO ₂	21.0	-16.0
<i>E_{X-endo}</i>	CH ₃	23.3	-3.3
	H	19.8	-9.8
	Cl	18.8	-6.9
	CN	17.4	-7.7
	NO ₂	16.9	-18.7

^a $\Delta G^\ddagger_{\text{sol}} = \Delta G^\ddagger_{\text{g}} + \Delta G^\ddagger_{\text{s}}$, where $\Delta G^\ddagger_{\text{s}}$ is the solvation energy difference in benzene between the TS and reactants. ^b $\Delta G^\circ_{\text{sol}} = \Delta G^\circ_{\text{g}} + \Delta G^\circ_{\text{s}}$, where $\Delta G^\circ_{\text{s}}$ is the solvation energy difference in benzene between the adduct and reactants.

to a decrease in the *endo* preference, as the electron-withdrawing power of substituent X increases (vide infra). This is also consistent with a reactivity increase due to a decrease in the FMO gap (Table 5) as the electron-withdrawing power of X increases along X = CH₃ → NO₂; i.e., the selectivity decreases as the reactivity increases in accordance with the reactivity–selectivity principle.¹⁷

Products Structures. All the products (with X = H) adopt half-chair conformations² (Figures 2 and 3) with the X (=H) atom in an equatorial position in two cases (*Z-endo* and *E_{X-exo}* products) and in an axial position in the other two cases (*Z-exo* and *E_{X-endo}* products). Although the reason the X (=H) group occupies equatorial or axial position is not clear, the equatorial X seems to stabilize the product by ca. 4 kcal mol⁻¹ more than the corresponding product with axial X (Table 2) due to reduced steric effect.

Solvent Effect. Solvent effects are calculated using the IPCM method at the isodensity level of 0.0004 au in benzene as shown in Table 7. The solvent effects are seen

(15) Reference 14, p 38.

(16) Hine, J. *Structural Effects on Equilibria in Organic Chemistry*; Wiley: New York, 1975; Chapter 3.

(17) (a) Pross, A. *Adv. Phys. Org. Chem.* **1977**, *14*, 69. (b) Buncl, E.; Wilson, H. *J. Chem. Educ.* **1987**, *64*, 475. (c) Lowry, T. H.; Richardson, K. S. *Mechanism and Theory in Organic Chemistry*, 3rd ed.; Harper and Row: New York, 1987; p 148.

to cause lowering of the barriers and reaction free energies almost uniformly so that there is no change in the relative order of ΔG^\ddagger depending on the substituent X. Since in the TS and product the charges on the dienophile, $^-\text{O}-\text{S}^+=\text{N}-\text{X}$, are delocalized, the solvation by benzene stabilizes the TS and product more than the reactants. This should lower the barrier heights and reaction free energies. The activation free energies of 17–24 kcal mol⁻¹ in benzene for X = CN and NO₂ in Table 7 are comparable to that for the cycloaddition of ethyl *N*-sulfinylcarbamate to 1,1'-bicyclohexenyl in benzene, $\Delta G^\ddagger = 19.8$ kcal mol⁻¹, in the temperature range 281.2–318.2 K.^{3a} Since it is more likely for the *E* and *Z* forms to equilibrate in solution,⁴ the cycloaddition may well proceed mainly by the lower barrier paths of the *E*-adduct formation.

In summary, the sulfinyl dienophiles are predominantly in *Z* forms rather than *E* forms in the ground state, and the energy difference decreases with the electron-withdrawing power of the X substituent on the N atom.

There are five factors which influence the energetic preference of the mode of adducts: (i) the $\sigma-\sigma^*$ secondary proximate charge-transfer interaction; (ii) the relative sizes of AO coefficients on S and N atoms in the LUMO of the dienophiles; (iii) steric hindrance of O and X toward the diene; (iv) the relative levels of the ground states and LUMOs of the dienophiles; (v) bond energies of the bonds (C–S and C–N) that are formed in the adducts. The *E_{X-endo}* adduct is preferred on account of the factors i and iii–v, (iii), but the *Z-exo* adduct is disfavored on account of i, iv, and v. In the *Z-exo* adduct, the larger LUMO AO coefficient on the S atom leads to the greater degree of *d*₅ bond formation relative to *d*₆, whereas, in the *E_{X-endo}* adduct, the $\sigma-\sigma^*$ secondary interaction leads to the greater degree of *d*₆ bond formation than *d*₅ in the TS.

Acknowledgment. Y.S.P. thanks the Korea Research Foundation for a postdoctoral fellowship.

JO991983P